

Electronic supporting Information (ESI)

Two novel $\mu_6\text{-O}^{2-}$ bridged $\text{Co}_{14}/\text{Ni}_{14}$ hydroxamate clusters packed in distorted face-centered cubic patterns

Yanping Zhang, Rui Lv, Jingyao Wang, Linyan Yang, Shengyun Liao, Jinlei Tian, Wen Gu,* Xin Liu*

Department of Chemistry, Collaborative Innovation Center of Chemical Science and Engineering, Nankai University, and Key Laboratory of Advanced Energy Materials Chemistry (MOE), Tianjin 300071, P. R. China. E-mail: guwen68@nankai.edu.cn, liuxin64@nankai.edu.cn

EXPERIMENTAL SECTION

Preparation of ligands.

The ligands sH₂bha and dppz (dipyrido[3,2-a:2',3'-c]phenazine) were synthesized via reported literature approach.¹

Synthesis of complexes 1 and 2.

The ligand sH₂bha (0.0216g, 0.1mmol) was deprotonated using triethylamine (40ul, 0.03mmol) in 10 ml of DMF. The aqueous solution of nickel nitrate hexahydrate (0.1 mmol) was added, which was stirred and refluxed for 1 h before dppz was introduced. Upon addition the ethanol solution of DPPZ, the solution changed from green to brown, the mixture was stirred and refluxed for another 2 h. the green solution is filtered, X-ray quality green single crystals were grown after allowing the filtrate to stand at room temperature undisturbed for four weeks. A similar synthetic procedure for Co₁₄ cluster was followed. In the case of Co₁₄ cluster, nickel nitrate hexahydrate was replaced by cobalt nitrate hydrate respectively.

¹ T. G. Barros, J. S. Williamson, O. A. C. Antunes and E. M. F. Muri, Letters in Drug Design & Discovery, 2009, 6, 186-192; A. Delgadillo, P. Romo, A. M. Leiva and B. H. Loeb, Chim. Acta, 2003, 86, 2110; M. Navarro, E. J. Cisneros-Fajardo, A. Sierralta, M. Fernandez-Mestre, P. Silva, D. Arrieché, and E. B. Marchan, Inorg. Chem., 2003, 8, 401.

Magnetic study

The magnetic susceptibility measurements of the polycrystalline samples were carried out over the temperature range of 2–300 K with a Quantum Design MPMS-XL 7 SQUID magnetometer using an applied magnetic field of 1000 Oe.

X-ray crystallography

Diffraction data for **1-2** were collected with a Bruker SMART APEX CCD instrument with graphite monochromatic Mo K α radiation ($\lambda = 0.71073 \text{ \AA}$). The data were collected at 113.15 K. The absorption corrections were made by multiscan methods. The structures were solved with the program Olex2 and refined by full matrix least-squares methods on all F^2 data with Shelxtl. All nonhydrogen atoms were refined anisotropically. Some bond distances connected with Br5 (Br5A), C59, C60 (C60A), C61 (C61A) in complex **1** and the planarity of C93-C98 (C93A-C98A) phenyl ring and Br9 (Br9A) in complex **2** were restrained because of their disorder. The SQUEEZE subroutine of the PLATON software suite was applied to remove the scattering from the highly disordered solvent molecules.² It is notable that the amount of disordered solvent deduced from the TGA results of **1** and **2** (nine DMF per formula unit of **1**, and seven DMF per formula unit of **2**) are not consistent with the squeezed structures (eight DMF per formula unit of **1**, and no DMF per formula unit of **2**). This is maybe due to the weak diffractions of these structurally disordered guest molecules in the structures. The crystallographic details are provided in Table 1.

Table S1. Crystallographic Data for complexes 1-2.

	1	2
Empirical formula	C ₁₄₅ H ₁₆₇ Br ₁₄ Co ₁₄ N ₂₈ O ₄₄	C ₂₄₄ H _{220.54} Br ₂₈ Ni ₂₈ N ₄₀ O ₇₄
Formula weight	4949.82	8788.49
Temperature	113.15 K	113.15 K
Crystal system	orthorhombic	triclinic
space group	Aea2	P-1
a/ Å	19.020(4)	17.868(4)
b/ Å	30.995(6)	20.685(4)
c/ Å	31.396(6)	29.557(6)
α /°	90	83.25(3)
β /°	90	72.87(3)
γ /°	90	64.81(3)
Volume/ Å ³	18509(6)	9447(4)
Z	4	1
ρ (mg/mm ³)	1.776	1.543
F(000)	9812.0	4321.0
Theta range for data	2.828 to 55.792°	3.314 to 52.068°
Index ranges	-24<=h<=25, -40<=k<=27, - 40<=l<=41	-20 <= h <= 22, -25 <= k <= 24, -36 <= l <= 36
Reflections collected /	72315	83882
Independent reflections	21777 [R(int) = 0.0924]	36795[R(int) = 0.0828]
Data/restraints/parameters	21777/ 65 / 1151	36795/215/1918
Goodness-of-fit on F ²	1.065	0.998
Final R indexes [I>=2 σ (I)]	R1 = 0.0735, wR2 = 0.1634	R1 = 0.0922, wR2 = 0.2393
R indices (all data)	R1 = 0.1076, wR2 = 0.1807	R1 = 0.1736, wR2 = 0.2934
Largest diff. peak/hole / e	1.27 / -1.03	1.37/-1.60

Comparison of Co₁₄ and the reported Co₁₆ cluster

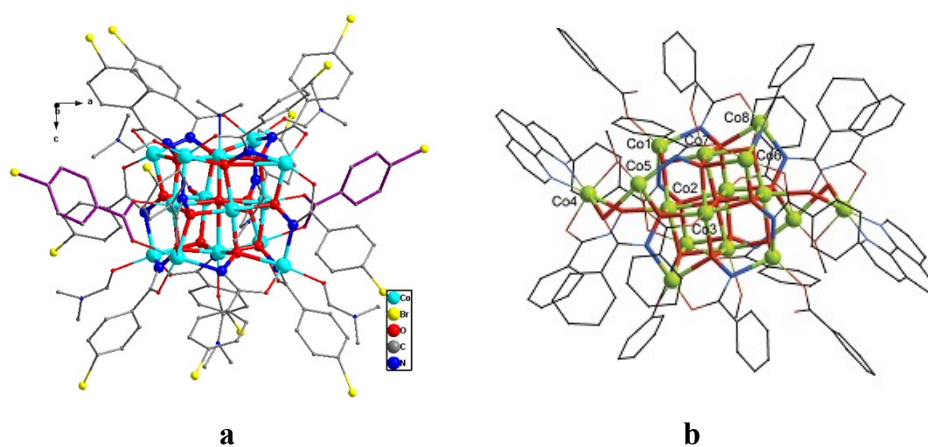


Fig. S1 (a) Perspective views of complex 1. (b) Perspective view of the reported Co₁₆ cluster.

The Co₁₄ cluster we synthesized is different from face-centered cube with two wings Co₁₆. i) Co₁₄ cluster crystallizes in the orthorhombic space group *Aba2* with *C*_{2v}-symmetry operation, while Co₁₆ cluster crystallizes in the triclinic *P-1* space group. ii) Synthetic routes are different. The Co₁₄ cluster is synthesized under reflux conditions, resulted in solutions from which we crystallize the cluster, while the reported Co₁₆ was synthesized via solvothermal techniques. iii) The coordination modes of the ligand are different. The hydroxamate ligand has only one coordination mode in Co₁₄ cluster, while there are three kinds of coordination modes in Co₁₆ cluster. iv) Two 1,10-phenanthroline molecules exist in Co₁₆ cluster.

Additional Structure Description

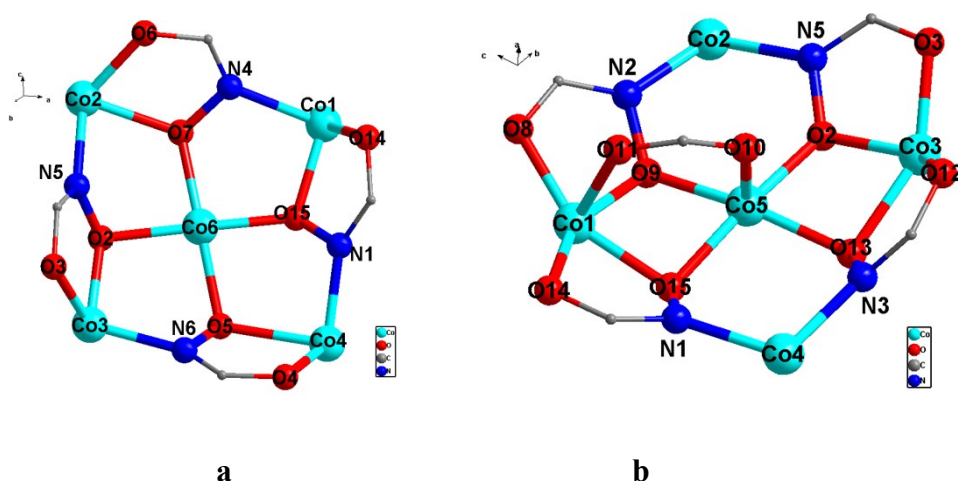


Fig. S2 (a) and (b) Salver-like faces of the FCC structure. Color key: Co, sky blue; O, red; N, blue; C, grey; Br, yellow. H atoms omitted for clarity.

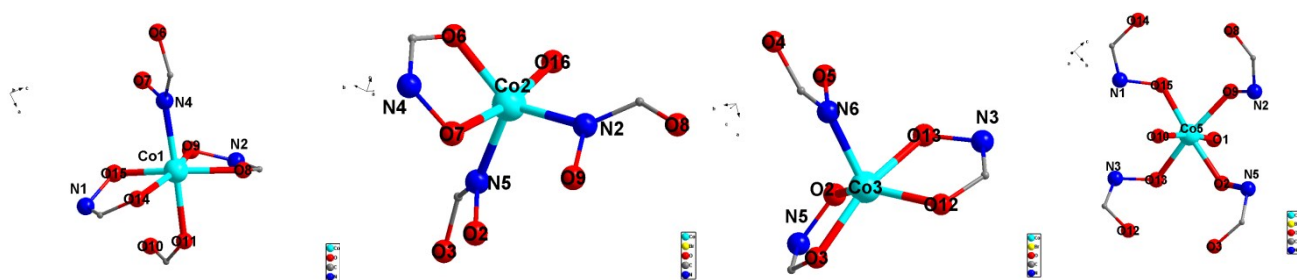


Fig. S3 (a) Coordination environments of the metal atoms of complex **1**; Color key: Co, sky blue; O, red; N, blue; C, grey. H atoms omitted for clarity.

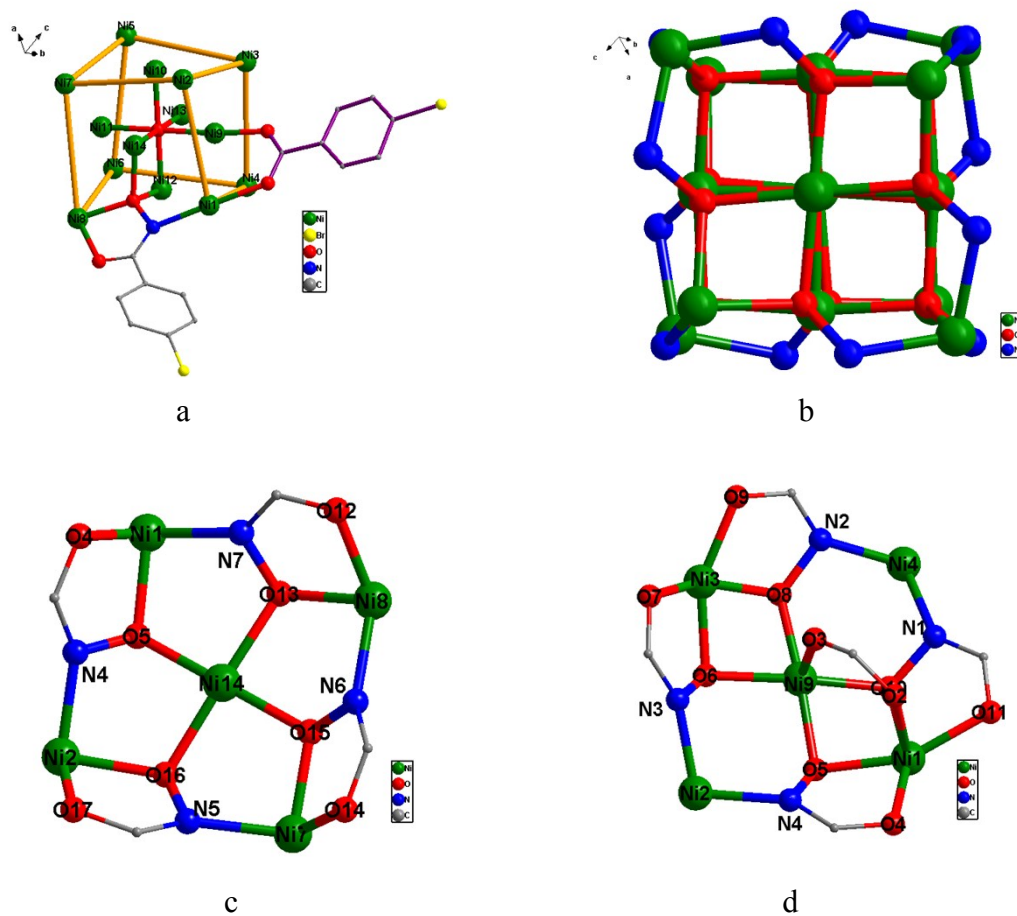


Fig. S4 (a) Views of structure of complex **2** with only one sbha and one sba bridging ligands shown for clarity. (b) Perspective views of the core structure of complex **2**. (c) and (d) salver-like faces of the FCC structure. The color of the bonds of sba ligands is violet. Color key: Ni, green; O, red; N, blue; C, grey; Br, yellow.

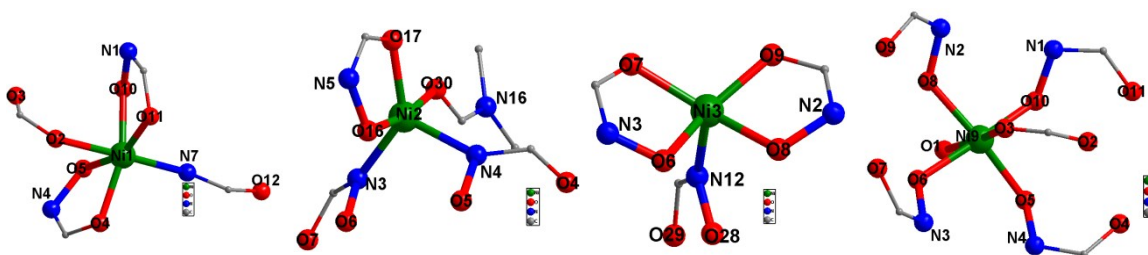


Fig. S5 Coordination environments of the metal atoms of complex **2**; Color key: Ni, green; O, red; N, blue; C, grey. H atoms omitted for clarity.

The coordination environment of Ni3 and Ni7 is $[\text{NiO}_4\text{N}]$, provided by four oxygen atoms from two sbha ligands and one nitrogen atom from one sbha ligand. The five-coordinated Ni2, Ni4, Ni5, Ni8 connect two oxygen atoms from one sbha ligand, two nitrogen atoms from two sbha ligands, and one oxygen atom from DMF, resulting in a distorted $[\text{NiO}_3\text{N}_2]$ trigonal bipyramidal coordination geometry. The six-coordinated Ni1 and Ni6 connect with four oxygen atoms from two sbha ligands, one nitrogen atom from one sbha ligand and one oxygen atom from sba ligand, resulting in a distorted $[\text{NiO}_5\text{N}]$ octahedral coordination geometry. Ni9-Ni14 atoms have similar distorted octahedral coordination environments, they connect with four oxygen atoms from four sbha ligands, one ($\mu_6\text{-O}^{2-}$) and one oxygen from sba ligand or DMF. The Ni-N (sbha) and Ni-O (sbha) separations span the range 2.026~2.142 Å and 1.959~2.183 Å. The average Ni-O ($\mu_6\text{-O}^{2-}$) bond distance is 2.159 Å. The average Ni-O (sba) bond distance is 2.093 Å. The Ni-O (DMF) bond distance span the range 2.029~2.054 Å.

Field-dependent magnetizations, Curie-Weiss plots of magnetic data, Cyclic voltammogram, Electronic absorption spectra, X-ray powder diffraction, IR spectroscopy and thermogravimetric analysis of complexes 1 and 2

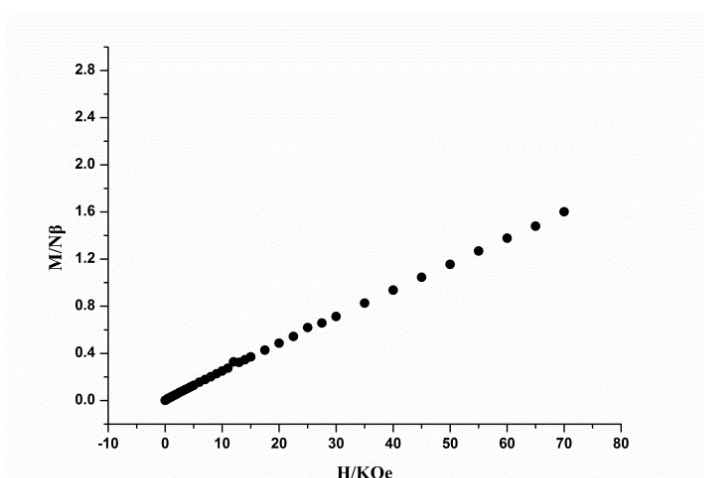


Fig. S6 Field dependence of magnetization for complex **2**

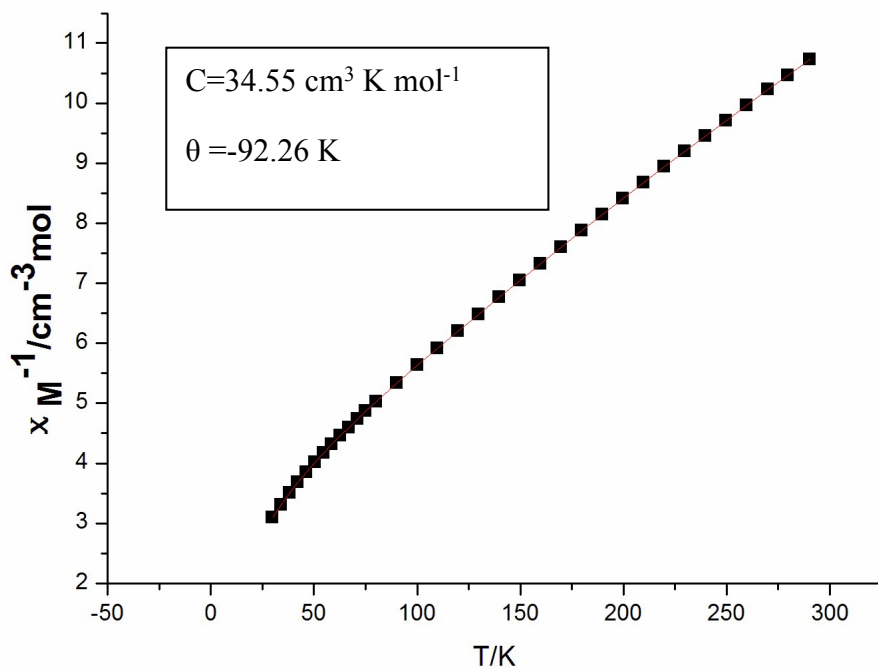


Fig. S7 Plot of $1/\chi$ against T for Co_{14} cluster.

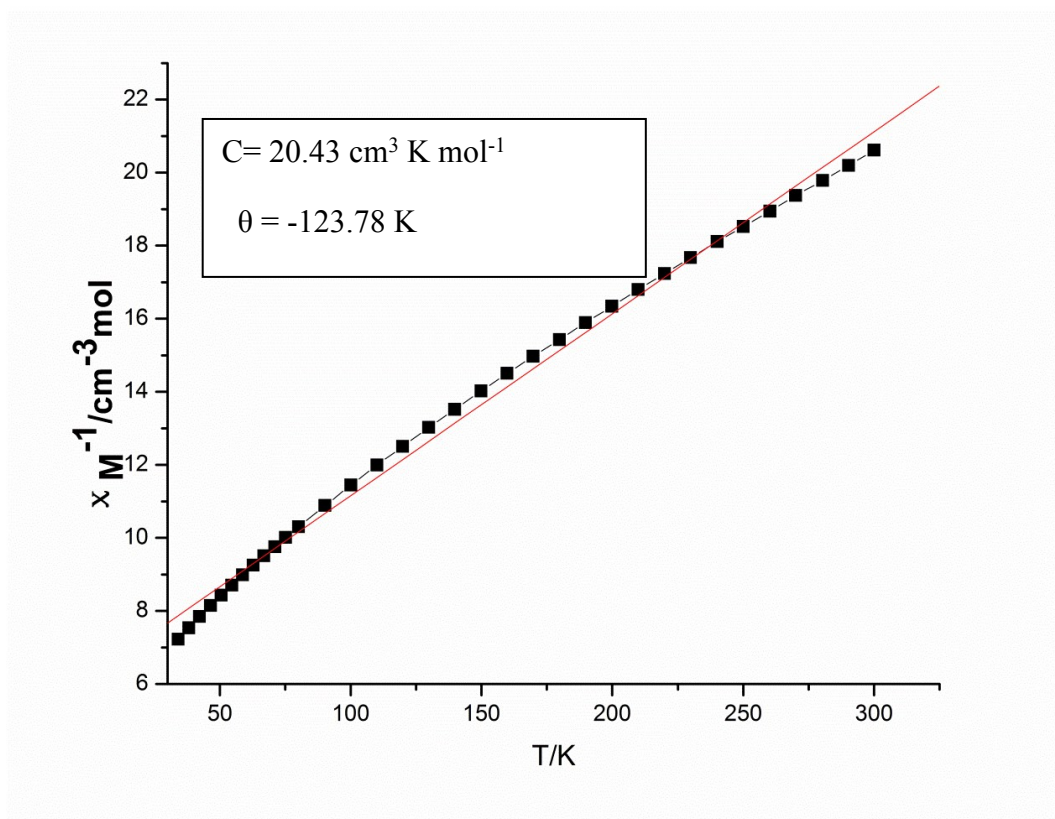


Fig. S8 Plot of $1/\chi$ against T for Ni_{14} cluster.

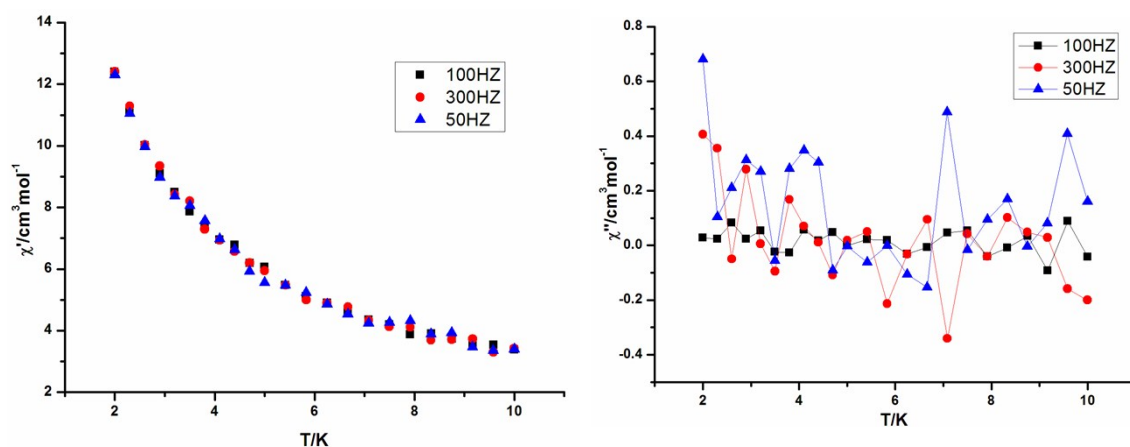


Fig. S9 In-phase and out-of-phase ac magnetic susceptibilities for complex **1**

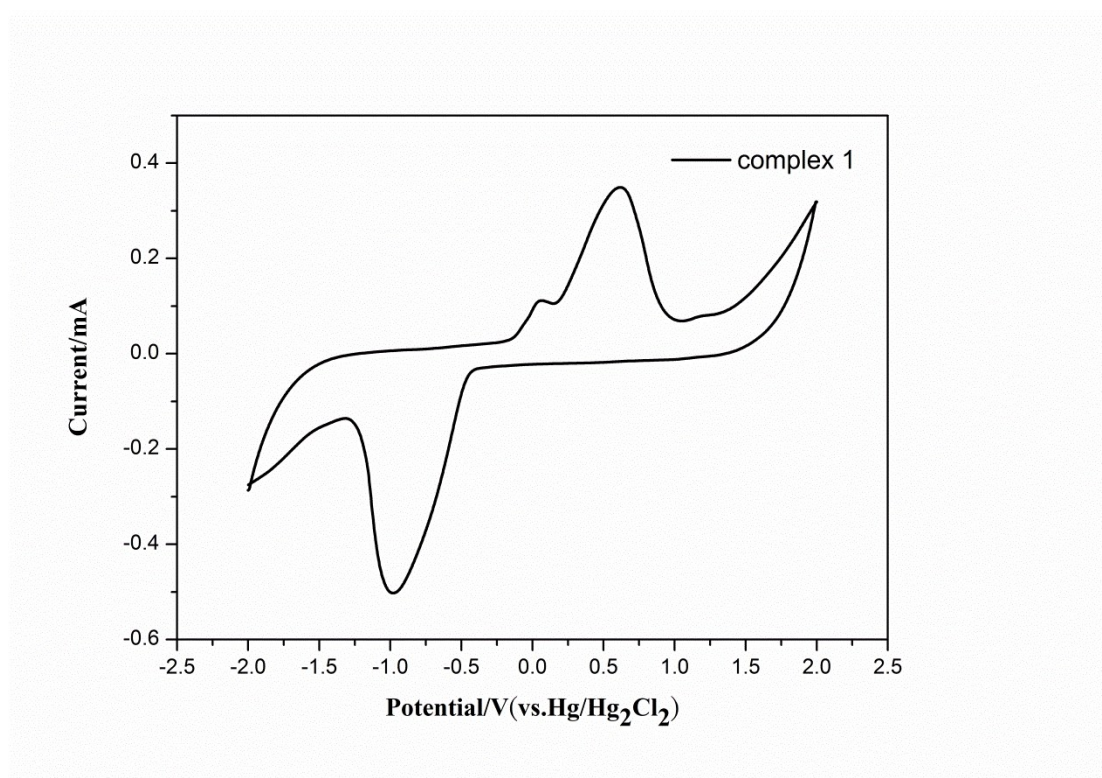


Fig.S10 The cyclic voltammogram of **1** in CH_2Cl_2 containing 0.1 M $n\text{-Bu}_4\text{NPF}_6$ with scan rate = 100 mV/s.

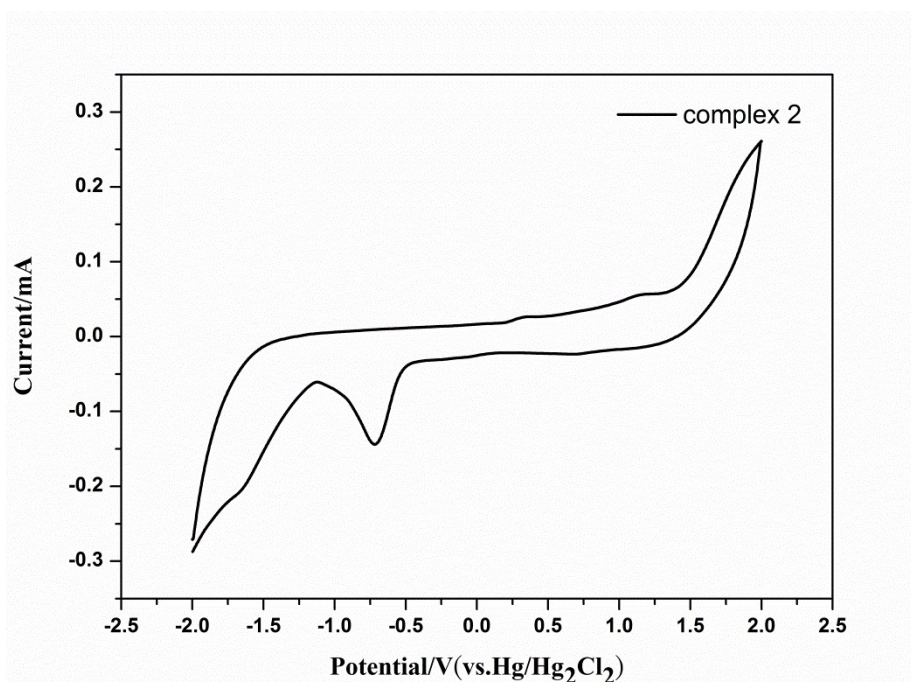


Fig.S11 The cyclic voltammogram of **2** in CH_2Cl_2 containing 0.1 M $n\text{-Bu}_4\text{NPF}_6$ with scan rate = 100 mV/s.

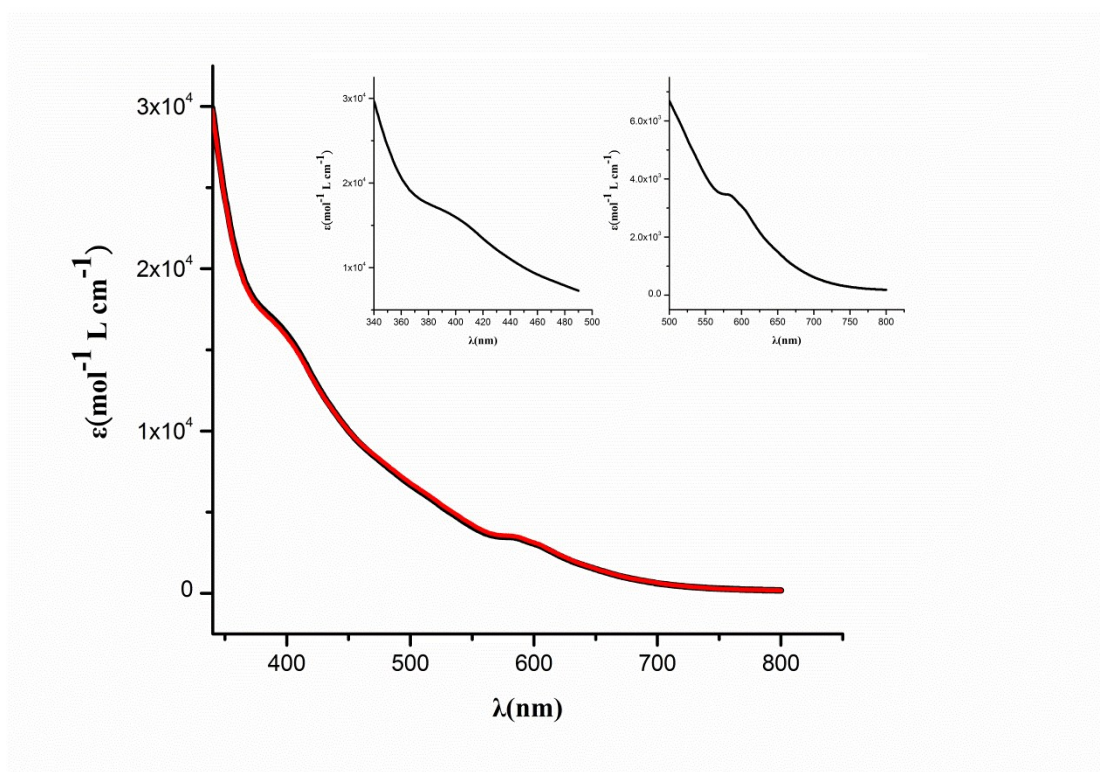


Fig.S12 Electronic absorption spectra of **1** in CH_2Cl_2 (black line) and CH_2Cl_2 / 0.1 M $n\text{-Bu}_4\text{NPF}_6$ (red line).

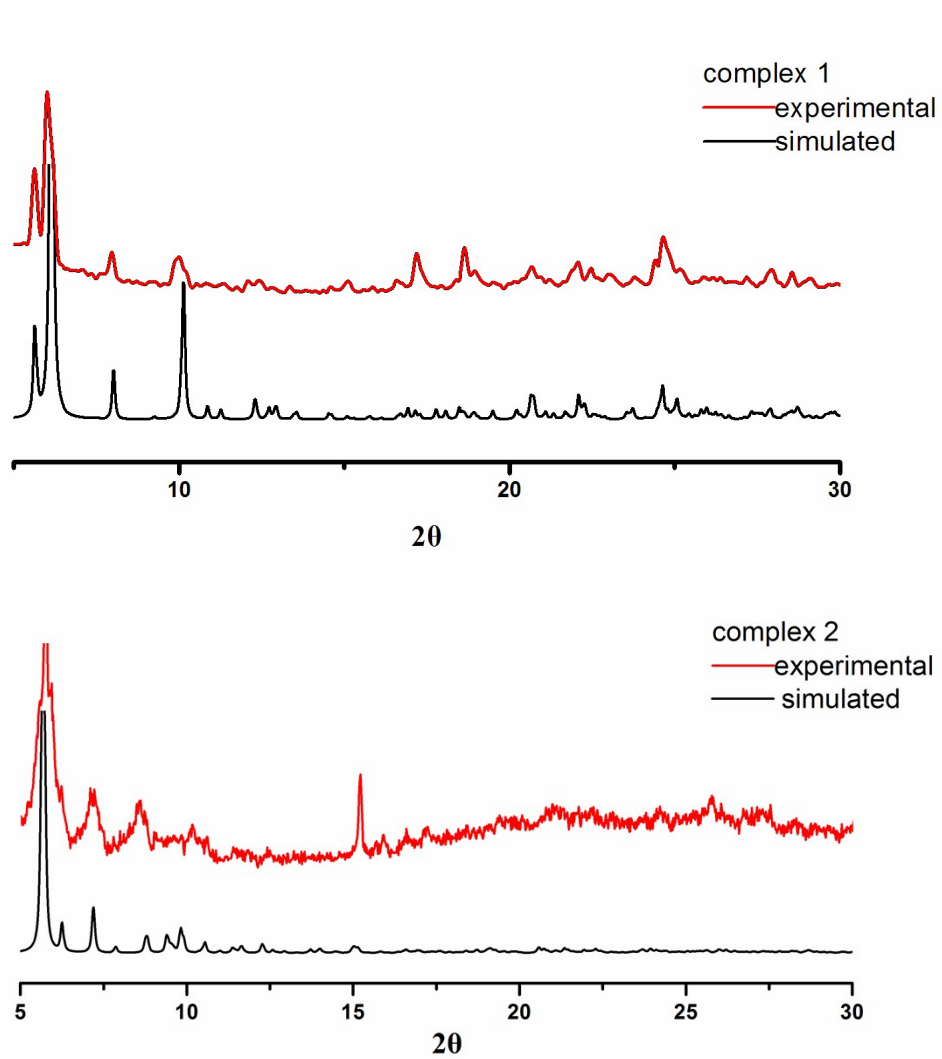


Fig. S13 The experimental and simulated XRPD diffraction pattern of complex **1** and **2**.

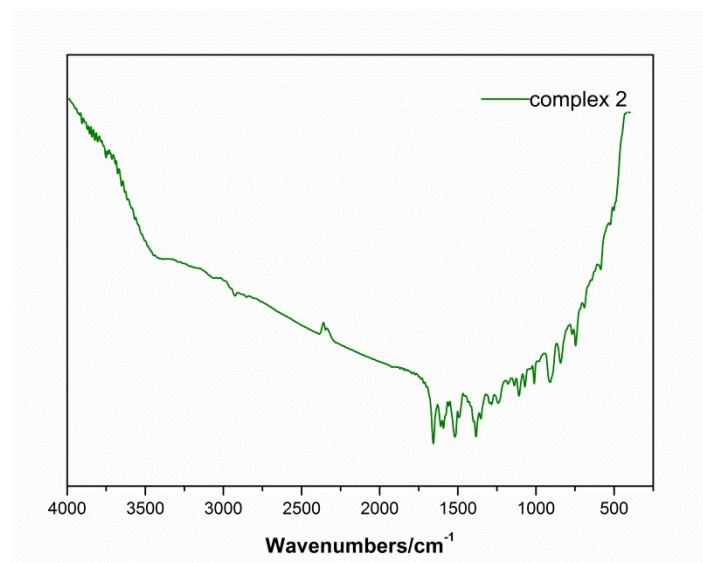
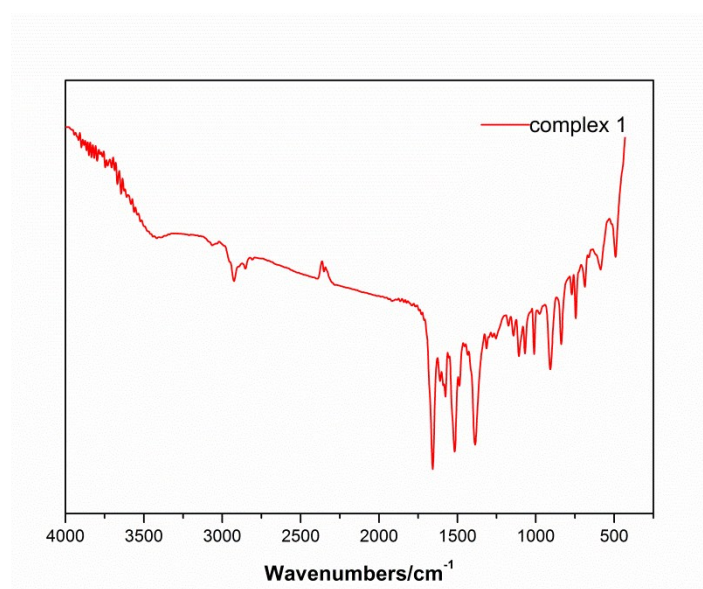
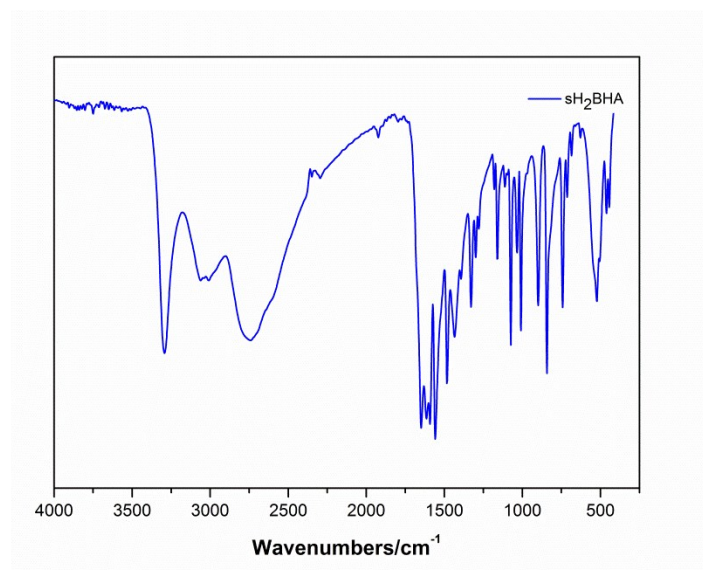


Fig. S14 Infrared spectrum of sH₂bha, complex 1 and 2

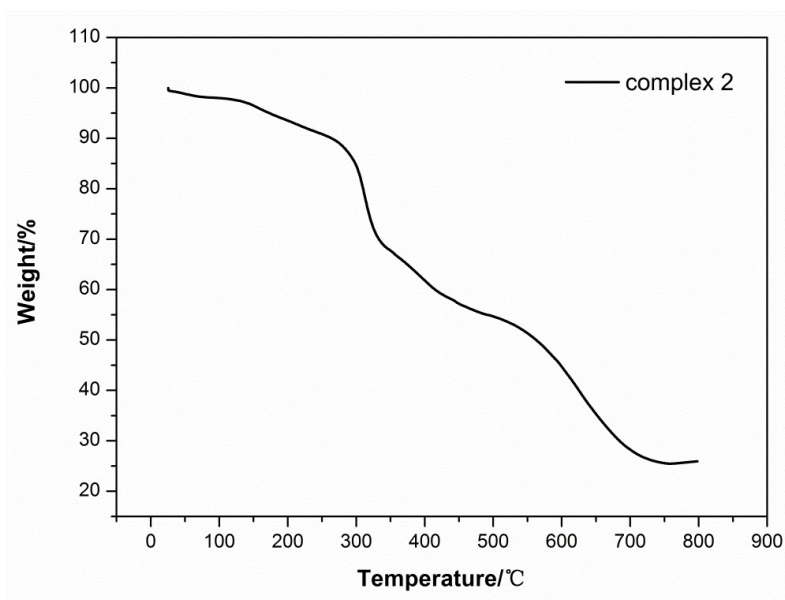
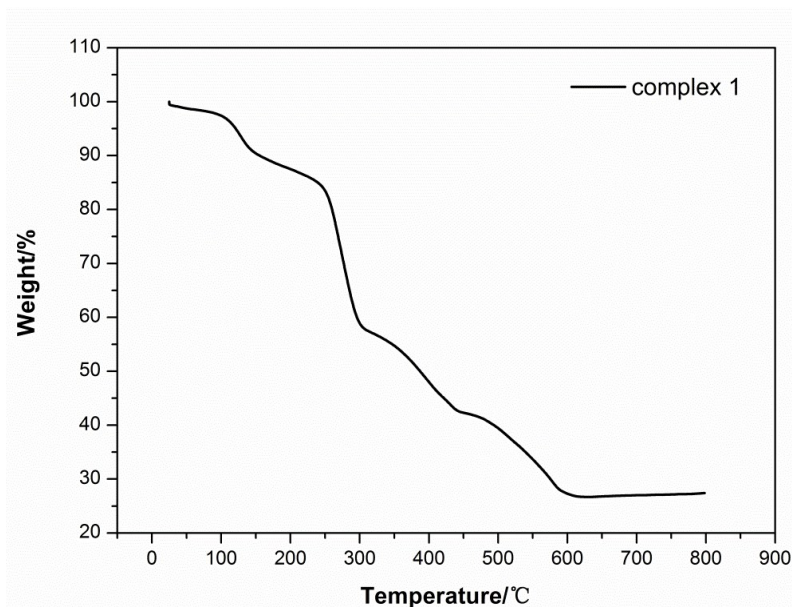


Fig. S15 Thermogravimetric analyses (TGA) of complex **1** and **2**

Thermogravimetric analysis of complex **1** indicates weight losses of 13% from 30 to 200 °C, which corresponds to the loss of eight DMF guest molecules (calc. 11.8%). Complex **2** indicates weight losses of 6% from 30 to 200 °C. It is notable that the amount of disordered solvent deduced from the TGA results of **1** and **2** (nine DMF per formula unit of **1**, and seven DMF per formula unit of **2**) are not consistent with the squeezed structures (eight DMF per formula unit of **1**, and no DMF per formula unit of **2**). This is maybe due to the weak diffractions of these structurally disordered guest molecules in the structures.